General and Comparative Endocrinology 331 (2023) 114179

Contents lists available at ScienceDirect

General and Comparative Endocrinology

journal homepage: www.elsevier.com/locate/ygcen

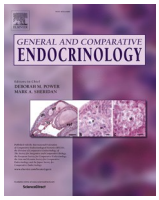

Development and metamorphosis in frogs deficient in the thyroid hormone transporter MCT8

Zachary R. Sterner [a], Ayah Jabrah [a], Nikko-Ideen Shaidani [b], Marko E. Horb [b], Rejenae Dockery [a], Bidisha Paul [a], Daniel R. Buchholz [a,*]

[a] Department of Biological Sciences, University of Cincinnati, Cincinnati, OH, United States
[b] Eugene Bell Center for Regenerative Biology and Tissue Engineering and National Xenopus Resource, Woods Hole, MA, United States

ARTICLE INFO

Keywords:
Xenopus laevis
CRISPR/Cas9
Monocarboxylate transporter 8
Slc16a2 knockout
Thyroid hormone transporter

ABSTRACT

Precisely regulated thyroid hormone (TH) signaling within tissues during frog metamorphosis gives rise to the organism-wide coordination of developmental events among organs required for survival. This TH signaling is controlled by multiple cellular mechanisms, including TH transport across the plasma membrane. A highly specific TH transporter has been identified, namely monocarboxylate transporter 8 (MCT8), which facilitates uptake and efflux of TH and is differentially and dynamically expressed among tissues during metamorphosis. We hypothesized that loss of MCT8 would alter tissue sensitivity to TH and affect the timing of tissue transformation. To address this, we used CRISPR/Cas9 to introduce frameshift mutations in *slc16a2*, the gene encoding MCT8, in *Xenopus laevis*. We produced homozygous mutant tadpoles with a 29-bp mutation in the L-chromosome and a 20-bp mutation in the S-chromosome. We found that MCT8 mutants survive metamorphosis with normal growth and development of external morphology throughout the larval period. Consistent with this result, the expression of the pituitary hormone regulating TH plasma levels (*tshb*) was similar among genotypes as was TH response gene expression in brain at metamorphic climax. Further, delayed initiation of limb outgrowth during natural metamorphosis and reduced hindlimb and tail TH sensitivity were not observed in MCT8 mutants. In sum, we did not observe an effect on TH-dependent development in MCT8 mutants, suggesting compensatory TH transport occurs in tadpole tissues, as seen in most tissues in all model organisms examined.

1. Introduction

Frog metamorphosis comprises a highly coordinated series of developmental events converting an aquatic, herbivorous tadpole into a terrestrial, carnivorous juvenile frog (Dodd and Dodd, 1976; Shi, 1999). Improper timing of any of these developmental events with respect to each other could result in death from dysregulated changes. For example, to ensure continuous locomotor ability, the limbs grow and develop first and then the tail resorbs. In the intestine, a gap in digestive ability occurs during metamorphosis when the skeletal feeding apparatus and intestine and pancreas are remodeled from the larval to adult versions (Ishizuya-Oka, 2017; Mukhi et al., 2008). Neural control systems must adjust appropriately to accommodate the changes in locomotion and feeding (Combes et al., 2021). Even though the initiation and overall rate of these developmental changes can be influenced by environmental conditions (Denver, 2009; Denver, 2017), the order of developmental events with respect to each other are more or less maintained.

Communication among tissues during metamorphosis regarding coordination of the timing of their metamorphic transformations does not occur. Tissues can undergo metamorphic change when isolated in culture and treated with TH (Baker and Tata, 1992; Ishizuya-Oka and Shimozawa, 1994). Also, *in-vivo* inhibition of TH signaling by use of transgenic overexpression of a dominant negative TH receptor in any one tissue does not affect the metamorphic changes in the other tissues (Brown et al., 2005). Rather than via tissue-tissue communication, the coordination of timing of tissue transformations during metamorphosis arises from a twofold mechanism involving 1) dynamic developmental profile of plasma TH during metamorphosis and 2) differential tissue sensitivity / responsivity to circulating TH levels. Plasma TH level rises from minimal in premetamorphic tadpoles to a peak at metamorphic climax and serves to regulate the overall initiation and rate of metamorphosis (Leloup and Buscaglia, 1977). All tissues experience the same changing blood plasma TH levels but initiate their metamorphic changes

* Corresponding author at: Department of Biological Sciences, University of Cincinnati, 711A Rieveschl Hall, 312 Clifton Ct, Cincinnati, OH 45221, United States.
E-mail address: buchhodr@ucmail.uc.edu (D.R. Buchholz).

https://doi.org/10.1016/j.ygcen.2022.114179
Received 18 August 2022; Received in revised form 14 November 2022; Accepted 19 November 2022
Available online 22 November 2022

at different time points specific to each tissue, i.e., limbs first and tail last, due to tissue sensitivity / responsivity to circulating TH levels as they increase (Shi et al., 1996). Tissues more sensitive to TH initiate their transformation earlier than other tissues because they can respond to lower plasma TH levels.

A major mechanism controlling tissue sensitivity is transport of TH across the cell membrane (Groeneweg et al., 2020). TH is a charged small molecule derived from two tyrosine amino acids linked together and thus does not pass through the cell membrane efficiently without protein assistance. Numerous transporters capable of facilitating TH transport exist, including LAT1, OATP1c1, and MCT8 (Kinne et al., 2011). MCT8 is the most specific TH transporter identified with a high specificity for T4 and T3, the prohormone and active versions of TH, respectively (van Geest et al., 2021). In *Xenopus*, MCT8 facilitates diffusion as both influx and efflux are facilitated (Mughal et al., 2017). Most tissues express many types of TH transporters, and thus each tissue has tissue-specific dependence on MCT8 for TH entrance into the cells and thus for amount of TH signaling (Choi et al., 2015; Connors et al.; 2010; Visser et al., 2010). The importance of TH transport in general and MCT8 in particular has been shown by MCT8 deficiency in humans, which causes a severe neurodevelopmental disorder characterized by impaired walking ability, intellectual disability, lack of speech, poor head control, and underweight (van Geest et al., 2021). A key aspect of the disease involves impaired TH entry via the blood brain barrier and consequent reduced TH signaling on some neurons and oligodendrocytes. MCT8 deficiency in zebrafish mimics many of the behavioral defects seen in human patients (Campinho et al., 2014; de Vrieze et al., 2014; Vatine et al., 2013). Surprisingly, mouse MCT8 knockout animals have no psychomotor defects (Salveridou et al., 2020). The difference between human and mouse appears to be the expression of OATP1c1 at the blood brain barrier in mice and not humans allowing mice to compensate for the loss of MCT8 (Bernal et al., 2015).

Compared to the other vertebrate models, the role of TH in frog development is more dramatic and more widespread among tissues, i.e., more tissues change and to a greater degree in response to TH during their aquatic to terrestrial transition (Just et al., 1981). Thus, one may predict that altered TH signaling, such as from lack of MCT8, may have a greater effect in frogs than other models because all tissues require precise timing and thus have a higher degree of dependency on proteins regulating TH sensitivity. In particular, previous studies have shown that hind limbs, which are among the first tissues to initiate metamorphosis, express high levels of MCT8 thus the timing of their metamorphic outgrowth may be affected by MCT8 mutation (Choi et al., 2015; Connors et al., 2010). On the other hand, because tissues are so dependent on TH, there may be increased compensatory or back-up mechanisms to ensure the proper amounts of TH signaling occurs at the right times among tissues, as seen in mouse brain (Salveridou et al., 2020). To examine the effect of MCT8 deficiency on frog metamorphosis, we produced MCT8 knockout frogs and examined their survival, TH-dependent growth and development, TH response gene expression, and tissue sensitivity to TH.

2. Materials and methods

2.1. CRISPR-Cas9 editing

To create MCT8 knockout frogs, CRISPR-Cas9 was used to target exon 1 of the *slc16a2* gene on both the L and S chromosomes of J-strain *X. laevis*. The sgRNA target (5′-AGGGGTCGGGTGCCCGACGGAGG-3′) was identified using CRISPRscan (Moreno-Mateos et al., 2015). The 5′ adenine nucleotide was modified to a guanine for improved mutagenesis (Gagnon et al., 2014). *In-vitro* transcription of the sgRNA PCR template using the SP6 MEGAscript kit (Ambion, Cat. No. AM1330) was used to synthesize the sgRNA. One-cell J-strain embryos (RRID: NXR_0024) were injected with 750 pg of the sgRNA and 1500 pg of Cas9 protein.

2.2. Husbandry and mating

Five F0 females were outcrossed with a J-strain male via *in vitro* fertilization to confirm the presence of germline mutations. Females were given 50 IU of pregnant mare serum gonadotropin (Bio Vender, Cat. No. RP17827210000) and 500 IU of human chorionic gonadotropin (Bio Vender, Cat. No. RP17825010) (Wlizla et al., 2018). Individual embryos were genotyped by isolating genomic DNA using Sigma-Aldrich GenElute Mammalian Genomic DNA Miniprep Kit (G1N350-1KT). PCR amplification of the targeted region was done using the following primers: L-chromosome forward primer 5′-AAGTGTAGCGAGCAGTGTGC-3′ and L-chromosome reverse primer 5′-TGGTCCTTTTAGGTTTCAGC-3′; S-chromosome forward primer 5′-CCAAGGGAGGGAGCAGTAGG-3′ and S-chromosome reverse primer 5′-GCACTACAGCAGGAATCCCT-3′. PCR products were purified using the NucleoSpin PCR Clean-up procedure (Macherey-Nagel 740609.250), and mutations were confirmed by Sanger sequencing. Three of the 5 F0 individuals were found to have F1 offspring with germline mutations. One F0 (female 5) had offspring with an out of frame mutation on both the long and short chromosome (L: −29 bp, S: −20 bp). 29 F1 offspring from female 5 were raised to adulthood in the National *Xenopus* Resource adhering to previously published X*enopus laevis* diet and water parameters (McNamara et al., 2018; Shaidani and McNamara, 2020). 21 of the 29 individuals were found to have mutations on the L alloallele, and 12 of the 29 F1s were found to have mutations on the S alloallele. Only 3 of the F1s had an out of frame mutation on both the long and short chromosome (L: −29 bp, S: −20 bp). The L:−29/+ S:−20/+ (*Xtr. slc16a2*^{em1Horb}, RRID:NXR_2001) *slc16a2* mutants are available from the NXR (https://www.mbl.edu/xenopus).

2.3. Heterozygote crosses and genetic screening by HMA

F2 adults that were heterozygous for the MCT8 mutation on the L-chromosome and homozygous for the MCT8 mutation on the S-chromosome, designated as Llss × Llss, were sent from the National Xenopus Resource (Pearl et al., 2012) to the University of Cincinnati and crossed. The F3 individuals were reared for 3 weeks and then genotyped using the heteroduplex mobility assay (HMA) (Naert and Vleminckx, 2018). Briefly, genomic DNA was prepared from tail tips by means of the HotSHOT protocol used in mice (Truett et al., 2000), where tadpole tail tips were excised using a razor blade and incubated in 50 μL of 25 mM NaOH/0.2 mM EDTA for 15 min at 95C, and then 50 μL of 40 mM Tris-HCl was added to neutralize the solution followed by vortexing. Polymerase chain reaction (PCR) (DreamTaq, Thermo Fisher) was then carried out using 1μL of the neutralized solution containing genomic DNA using primers to amplify a 260-bp region surrounding the CRISPR target site. The forward and reverse primers, which bind to both the L- and S- chromosomes, were: 5′-GAAGAGCAGGGGATGCGG-3′ and 5′-TGAAGTCCATGCCCTTGTCCC-3′. DNA strands were then separated and allowed to reanneal in the PCR machine (95C for 5 min, 16C for 10 min, and 25C for 5 min). These reactions were loaded on 8 % polyacrylamide gels and run at 150 V. Gels stained with ethidium bromide were imaged using a UV transilluminator gel imager. Tadpoles were sorted into genotypes based on their HMA patterns and used in experiments. The use of the F2 and F3 animals was in accordance with approved guidelines of the University of Cincinnati Institutional Animal Care and Use Committee (IACUC protocol # 06–10-03–01).

2.4. Growth and development

When the F3 tadpoles were 21 days old, 79 individuals were staged then genotyped using HMA to assess the effect of the mutation on the initiation of limb outgrowth. Additional F3 tadpoles were genotyped using HMA at Nieuwkoop and Faber (NF) stage 50–53 (premetamorphosis), reared to NF 54 (end of premetamorphosis), and then individually reared in 2 L buckets (n = 10 per genotype) until NF66 (tail

resorption, end of metamorphosis) (Nieuwkoop and Faber, 1994). Tadpoles were fed Sera micron food *ad lib*. daily with water changes occurring every 3 days. All tadpoles were reared on the same shelf level, and buckets were shifted to different positions randomly across the shelf each day to minimize effects of slight temperature variation across the shelf (<2 degrees Celsius). NF stage and snout-vent length (from anterior-most point of head not including tentacles to posterior part of abdomen) were recorded for each tadpole every 5 days until tail resorption. Tadpoles were also checked daily to record the day they reached NF 58 (mid-metamorphosis), NF 62 (metamorphic climax), and NF 66 (complete tail resorption).

2.5. Hormone treatments, tissue harvest, and quantitative PCR

To measure tissue sensitivity to TH among genotypes, F3 tadpoles were genotyped with HMA at NF 50–53, reared to NF 54, and treated with 0, 0.5, 2, or 5 nM tri-iodothyronine (T3, the active form of TH) for 24 hrs prior to tissue harvest of tail and hindlimbs, n = 10 per genotype. To assess effect on thyroid stimulating hormone mRNA expression, whole brains including pituitary from genotyped F3 tadpoles were harvested at NF 62. At tissue harvest, tadpoles were anesthetized in buffered MS222, then tissues were collected, snap frozen on dry ice, and stored at −80 degrees Celsius as described (Patmann et al., 2017). RNA extraction was performed using TRI REAGENT RT following the manufacturer's instructions (Molecular Research Center, Inc.). Complementary DNA synthesis from 1 μg RNA for each sample was obtained using the High-Capacity cDNA reverse transcription kit (Applied Biosystems). Quantitative PCR (qPCR) was carried out using SYBR green master mix on a 7300 Real Time PCR System (Applied Biosystems) for Krüppel-like factor 9 (*klf9*) and TH receptor beta (*thrb*) on tails, hindlimbs, and brains and for thyroid stimulating hormone beta (*tshb*) on brains with gene-specific primers that spanned large introns to mitigate genomic DNA contamination (Table1). All qPCRs included a dissociation curve analysis to show that a single PCR product was produced. The reference gene ribosomal protein L8 (*rpl8*) was used (Dhorne-Pollet et al., 2013) and showed no significant differences among genotypes or treatments (data not shown). Relative quantification method ΔΔCt was used to compare expression levels of target genes normalized to *rpl8* (Livak and Schmittgen, 2001).

2.6. Statistical analysis

Data were checked for normal distribution using Shapiro Wilk test of normality. For normally distributed data, one-way or two-way full-factorial analysis of variance (ANOVA) was performed with base R (R Core Team, 2018). For analyses with significant effects, ANOVA was followed by pairwise comparisons using the Tukey-Kramer post hoc test to identify significant differences among treatments and genotype as part of the agricolae package in R. For data which did not follow normal distribution, non-parametric Kruskal-Wallis test was conducted in R followed by pairwise comparisons using Wilcoxon rank sum exact test in R.

Table 1
Gene-specific primers for TH response gene expression analysis.

Gene (L- and/or S-chromosome)	Primer sequence (5′ →3′)
thrb (both L and S)	F: AAGCCTTCAGCCAGTTTACA
	R: GAGCGACATGATCTCCATACAA
rpl8 (both L and S)	F: AGAAGGTCATCTCATCTGCTAAC
	R: GGATAGGTTTGTCAATACGACCA
klf9 (both L and S)	F: TACTGGGTGTGGCAAAGTTTAT
(F primer has 1 mismatch in S chromosome)	R: CTCTTCTCACAGAGTGGACATC
tshb (L only)	F: GTTCAGGATTCTGCATGACAAGG
	R: ACAGTCAGTGTAGCCAGTGTTA

3. Results

3.1. CRISPR design and mutant production

To generate an MCT8 knockout, we designed a sgRNA (5′-GGGGGTCGGGTGCCCGACGG-3′) that matches the sequence in the first exon of the *slc16a2* gene of both L- and S-chromosomes of J-strain *X. laevis* (Fig. 1). In humans there are two transcription start sites creating a long and short form of MCT8, but only the short form is found in human tissues to date, and the homologues of MCT8 in other vertebrates correspond to the short form (van Geest et al., 2021). In addition to the full-length, a truncated transcript of MCT8 occurs in mouse missing part of the first transmembrane helix, but no evidence exists for alternate MCT8 transcripts in humans, rats, chicken, frog, fish. Structure function studies indicate the first transmembrane helix is required for TH transport function, thus frameshift mutations in this region will disrupt the protein starting in the first transmembrane domain and are known to be disease causing in humans (Friesema et al., 2010; Kleinau et al., 2011).

We injected 40 embryos and raised them to adulthood. Once they reached sexual maturity, 5 F0 founders were outcrossed with J strain *X. laevis* to generate F1 offspring. Of the F0 founders, 3 produced offspring with germline mutations and 2 showed no germline transmission. We identified a 29-bp deletion in *slc16a2* on the L-chromosome and a 20-bp deletion in *slc16a2* on the S-chromosome in offspring from one of the founders (Fig. 1). Initial genotyping of a clutch of F1 embryos from this founder showed the L-chromosome has a 9-bp deletion polymorphism fairly near the sgRNA target site (deletes entire 5′ UTR). The L-chromosome from the male parent is heterozygous for the 29-bp deletion and does not have the 9-bp deletion, whereas the L-chromosome from the female parent is heterozygous for both the 9 bp 5′UTR deletion as well as the 29-bp deletion within the target site. Sequencing F2 embryos revealed that the 29-bp and 9-bp deletions are on separate chromosomes, indicating that the 9-bp deletion in the 5′UTR from the F0 female is its own small polymorphism rather than a result of the CRISPR injection and that it entered earlier in the genetic line when J-strain founders were crossed with an outcrossed wild-type individual, which is expected to carry more SNPs than J-strain frogs.

3.2. Survival of mutants

To analyze the effect of the *slc16a2* mutations on survival through embryogenesis and adulthood, we crossed an F1 male to an F1 female we designated as LlSs × LlSs, which indicates both parents were heterozygous for the 29-bp deletion in the L-chromosome and heterozygous for the 20-bp deletion in the S-chromosome. The F2 embryos were reared in three dishes of n = 100 embryos starting at the 4-cell stage. The average survival rate through Nieuwkoop and Faber (NF) stage 42 (just before initiation of feeding) was 91 %. Fifty of these tadpoles were then haphazardly chosen for rearing, and 39 survived to adulthood, all of which were then genotyped by sequencing. The proportions of observed genotypes matched the expected ratio and thus the mutations do not affect embryo nor adult survival rates (Table 2). Four individuals were double null indicating that complete lack of MCT8 is not lethal. In addition, all mutant animals appeared normal in size and behavior based on routine observation during husbandry.

3.3. Mutant growth and development

We next analyzed the effect of the *slc16a2* mutation on development in more detail. The most divergent phenotypes would be expected from comparing wild-type versus double homozygous mutant, i.e., LLSS vs llss, but to obtain siblings of these genotypes would require extensive screening of tadpoles from an LlSs × LlSs cross. To reduce screening effort, we decided to test three genotypes, namely LLss, Llss, llss, from an Llss × Llss cross. We compared these three because of the dominant

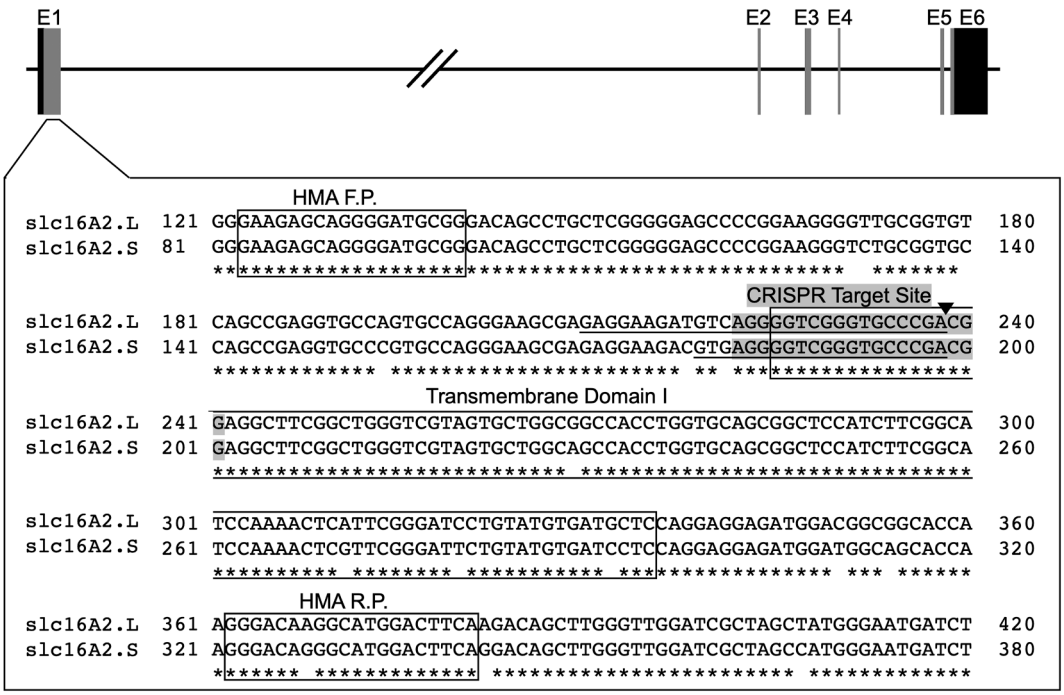

Fig. 1. CRISPR/Cas9 target site for *slc16a2*. The gene encoding MCT8, *slc16a2*, has 6 exons labeled E1-6, with the coding region shown as vertical grey bars and the 5′ and 3′ untranslated regions shown as vertical black bars. The DNA sequences from the L- and S-chromosomes around the CRISPR target site in Exon 1 are shown in the large, boxed area. Gaps in the asterisks below the *slc16a2.L* and *slc16a2.S* sequences show sequence divergence between the two *slc16a2* loci. The exact CRISPR target site, i.e., the sgRNA sequence, is shaded, and the Cas9 cut site is shown by the black triangle. The 29-base pair deletion in *slc16a2.L* and the 20-base pair deletion in *slc16a2.S* are underlined. The forward and reverse primers used in the heteroduplex migration assay (HMA F.P, HMA R.P) and the first transmembrane domain required for MCT8 function are boxed.

Table 2
Genotypes of animals reared to adulthood from LlSs cross.

L-chromosome	S-chromosome	n =	Expected %	Observed %
LL	SS	6	6.25	15.38
LL	Ss	4	12.5	10.26
LL	ss	2	6.25	5.13
Ll	SS	7	12.5	17.79
Ll	Ss	7	12.5	17.79
Ll	ss	7	12.5	17.79
ll	SS	0	6.25	0
ll	Ss	2	12.5	5.13
ll	ss	4	6.25	10.26
		Sum = 39	100 %	100 %

expression of *slc16a2* from the L-chromosome compared to the S-chromosome as seen in RNA-seq data from adult tissues available on XenBase (Fig. 2)(Karimi et al., 2018). The loss of the L allele is expected to be more severe than loss of the S allele due to its higher expression level and broader tissue distribution. Use of HMA to identify genotypes from the Llss × Llss cross was possible because, even though both L and S loci were PCR amplified for HMA, the resulting mixture of homoduplexes and heteroduplexes could unambiguously distinguish all three genotypes (Fig. 3).

To observe an effect of the MCT8 mutation on development, we used tadpoles of different *slc16a2* genotypes to examine the initiation and rate of TH-dependent development. Changes in rate of metamorphosis can be measured because of the potential for large dynamic range in metamorphic rate and because of the well-established finely divided developmental stages (Dodd and Dodd, 1976; Nieuwkoop and Faber, 1994). Rearing tadpoles individually under identical conditions allows for readily detectable differences between genotypes uninfluenced by potentially confounding interactions between individuals. We measured snout-vent length and recorded Nieuwkoop and Faber (NF) stage every five days from NF 56 to 66, i.e., from beginning of metamorphosis to tail resorption. The tadpoles had the same size and stage at the beginning of the experiment, and no significant difference in size or stage was observed among the three genotypes (Fig. 4A, B). A technique with more statistical power to detect differences among genotypes is to record the exact day that easily recognizable stages are obtained for each individual, which are day of forelimb emergence (NF58), metamorphic climax (NF62), and tail resorption (NF66). As before, we found no significant differences among genotypes in achieving these landmark stages (Fig. 4C, D, E).

3.4. Expression of tshb in pituitary and TH response genes in brain

In humans and mammalian knockout models of MCT8 deficiency, plasma levels of thyroid stimulating hormone beta (*tshb*) are normal or high normal, and in the zebrafish models of MCT8 deficiency, transiently low levels of *tshb* were observed (de Vrieze et al., 2014; Salveridou et al., 2020; van Geest et al., 2021). We measured *tshb* mRNA expression at climax of metamorphosis when TSH levels are normally high and found no significant difference in expression among genotypes (Fig. 5A). We also measured two TH-response genes, *klf9* and *thrb*, to compare degree of TH signaling in brain among genotypes because as with virtually all tadpole tissues, brain is responsive to TH (Denver et al., 1997). We found no significant differences among genotypes (Fig. 5B, C).

3.5. Tissue sensitivity to TH

A feature of developmental staging that may obscure an effect of an MCT8 mutation is that hindlimbs are used to assess the first stages of metamorphosis. Hindlimb outgrowth may be most affected by altered TH sensitivity from lack of MCT8 because hindlimb outgrowth is the first TH-dependent developmental event to occur and thus is very TH

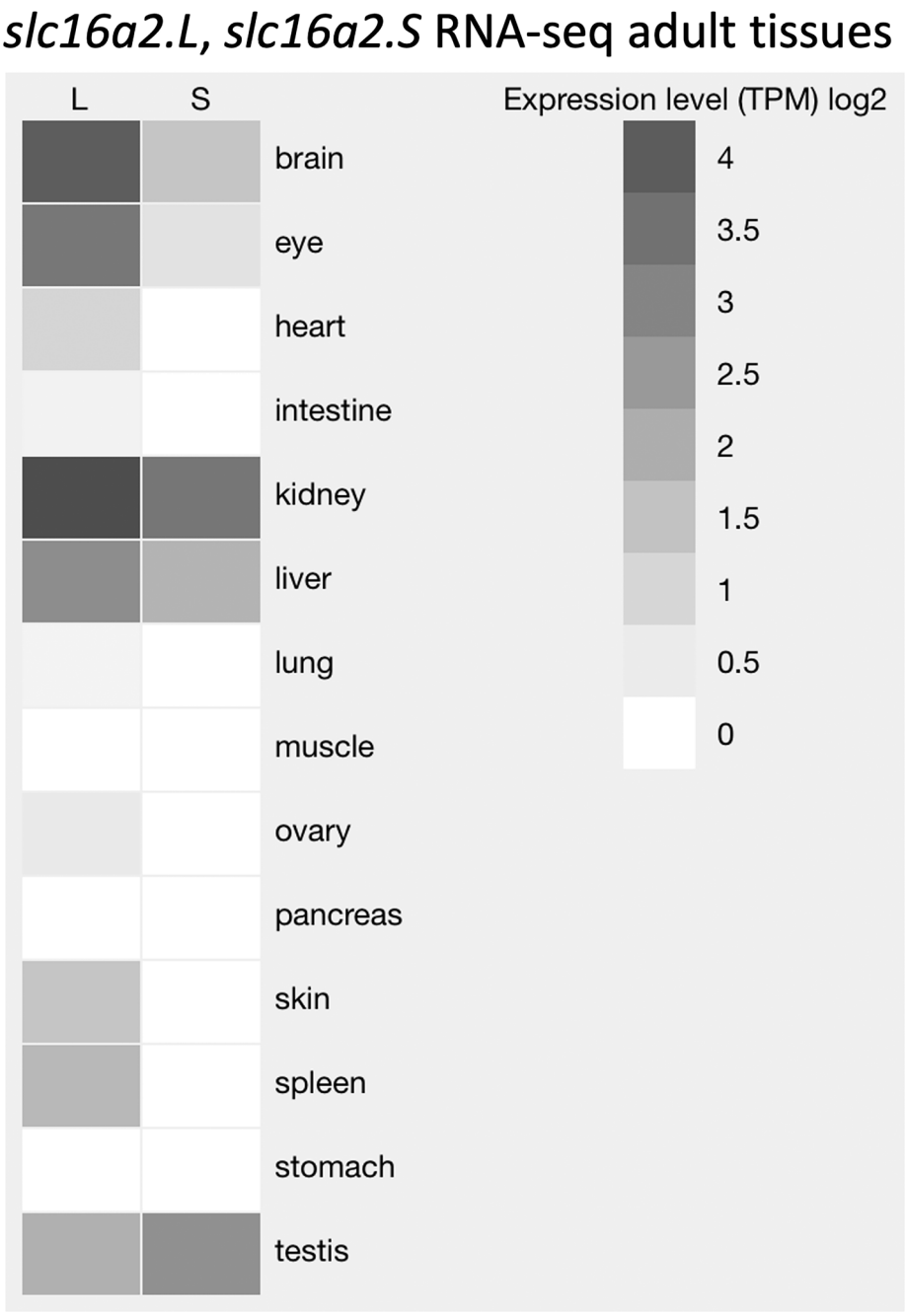

Fig. 2. Expression and tissue distribution of *slc16a2.L and slc16a2.S*. The expression levels of *slc16a2.L and slc16a2.S* among adult tissues of *X. laevis* are represented by shades of gray that indicate log2 of total counts per million (TCM) from RNA-seq data. This figure was obtained using the data visualization tool on XenBase (Karimi et al., 2018).

sensitive in order to respond when plasma TH levels are very low. Also, hindlimbs express MCT8 and other TH transporters typically at higher levels at early stages than other tissues (Connors et al., 2010). For example, it is possible that lack of MCT8 in hind limbs would make them less able to grow out compared to wild type and thus grow out when the plasma levels increased which by then the tadpoles would be a little bit larger. If we were just going by stage which is determined by limb outgrowth, we would not notice that such a difference was present. To account for this possibility, we measured hindlimb length and snout-vent length at a predetermined time to detect any effect of altered hind limb sensitivity to TH due to lack of MCT8. Specifically, we measured 79 haphazardly selected F3 tadpoles at 21 days when they typically start metamorphosis under our rearing conditions and genotyped them by HMA after measurement. We found no significant differences in body size or degree of limb outgrowth relative to body size among genotypes, indicating MCT8 had no effect on timing of limb outgrowth (Fig. 6).

To directly assess the effect of MCT8 loss on sensitivity to TH, we used two tissues with high MCT8 expression but highly divergent TH sensitivity, namely the tail and hindlimbs. We treated premetamorphic tadpoles with a range of low TH doses (0, 0.5, 2, 5 nM T3) and measured TH response gene induction. In tail, higher TH doses induced TH response genes more than the lower dose for *kfl9*, but there was no significant difference between mutant and wild type (Fig. 7 A). The 5 nM dose was not enough to significantly induce *thrb* in tail (Fig. 7B). The results for *klf9* in the hind limb were similar, but for *thrb*, mutant

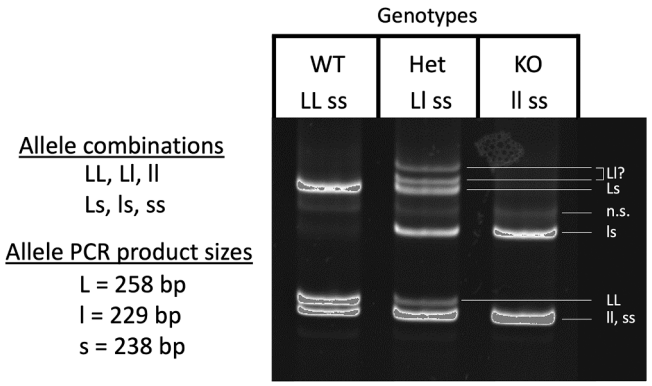

Fig. 3. *slc16a2* genotyping using the heteroduplex migration assay. All tadpoles used in the growth and development experiments were F3 offspring from the F2 cross Llss × Llss, where both parents were heterozygous for the MCT8 mutation on the L-chromosome and homozygous for the MCT8 mutation on the S-chromosome. The three possible genotypes from this cross were LLss, designated as "wild-type" (WT), Llss, designated as "heterozygous" (HET), and llss, designated as knockout (KO). PCR amplification of a DNA region around the CRISPR target site from each of these genotypes followed by melting and reannealing of the PCR products results in a total of 6 possible allele combinations, namely LL, ll, ss (homoduplexes) and Ll, Ls, ls (heteroduplexes). When run on an 8 % PAGE gel, the reannealed DNA homo- and heteroduplexes can be identified as shown on the gel image based on the allele PCR product sizes. Genotypes were assigned based on their unique set of bands on the gel. n.s. = non-specific.

hindlimbs exhibited significantly higher *thrb* induction at the highest TH dose compared to wild type (Fig. 7C and D).

4. Discussion

TH signaling is necessary and sufficient for frog metamorphosis, and virtually all tadpole tissues transform from the larval to the juvenile form under the control of TH (Shi, 1999; Shi, 2021). No other vertebrate is so comprehensively dependent on TH for its post-embryonic development (Just et al., 1981). Thus, one may hypothesize that tadpoles would be the most affected by mutations affecting TH signaling. On the other hand, because TH signaling is so critical for frog metamorphosis, tadpoles may have abundant compensatory mechanisms to alleviate mutations affecting TH signaling. To examine this issue for MCT8, the most specific TH transporter identified to date, we used CRISPR/Cas9 to target exon 1 of *slc16a2* encoding MCT8 in *X. laevis*. The frameshift mutations made here and the highly conserved sequence and function of MCT8 seen in vertebrates suggests the mutant tadpoles used in the current study completely lacked MCT8 function (Friesema et al., 2010; Groeneweg et al., 2019; Kleinau et al., 2011; Mughal et al., 2017).

A peculiarity to *Xenopus laevis* not common among vertebrates is that *X. laevis* is allotetraploid and thus has two genomic locations for MCT8, one on each set of duplicated chromosomes, i.e., L and S (Session et al., 2016). Mammals have one genomic location for this gene, and so does zebrafish which only retained one MCT8 locus even though it has an additional ancestral whole genome duplication with respect to tetrapods (Bradford et al., 2022). The related frog species *X. tropicalis* is diploid rather than tetraploid and thus has only one MCT8 genomic location rather than the two found in *X. laevis*, but husbandry for the genetically more tractable *X. tropicalis* is often more troublesome compared to *X. laevis* (Hellsten et al., 2010; Jafkins et al., 2012; McNamara et al., 2018). From these considerations, *X. laevis* was chosen, and thus both MCT8 loci required disruption to eliminate MCT8 function. We successfully disrupted both L and S MCT8 loci and produced double homozygous mutants. As seen in other species with MCT8 deficiency (Groeneweg et al., 2020; Salveridou et al., 2020; Vatine et al., 2013), the survival at the expected genotype frequency through embryogenesis, post-embryonic development, and adulthood occurred in double homozygous L and S MCT8 mutants in frogs.

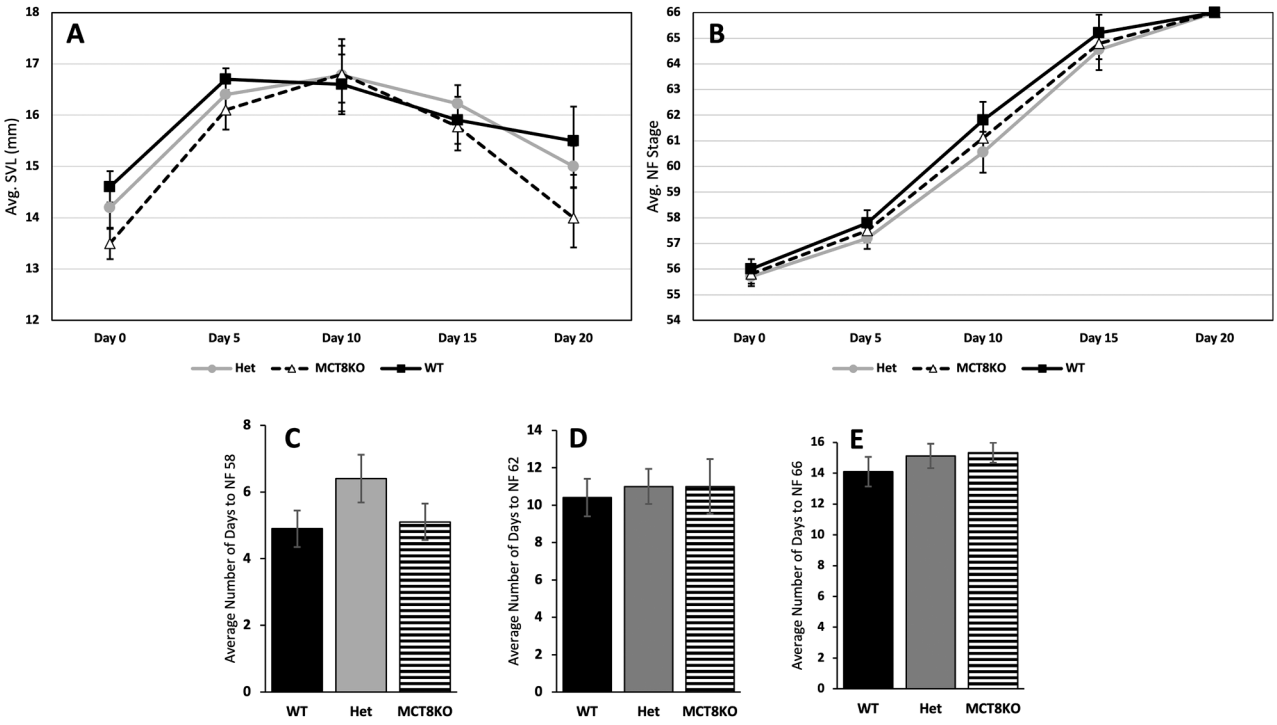

Fig. 4. Growth and development in MCT8 mutant tadpoles. Genotyped and individually reared tadpoles were (A) measured for snout-vent length (SVL) and (B) staged according to Nieuwkoop and Faber (NF) every 5 days starting at the beginning of metamorphosis (NF stage 54, limb bud outgrowth) to the end of metamorphosis (NF stage 66, complete tail resorption). In addition, tadpoles were monitored daily to record exact number of days after NF 54 to achieve (C) forelimb emergence (NF 58), (D) metamorphic climax (NF 62), and (E) tail resorption (NF 66). Means and standard error for each genotype are shown, n = 10 per genotype. WT = wild-type (LLss), Het = heterozygous (Llss), MCT8KO = homozygous knockout (llss). No statistical differences were found using one-way ANOVA, $p < 0.5$.

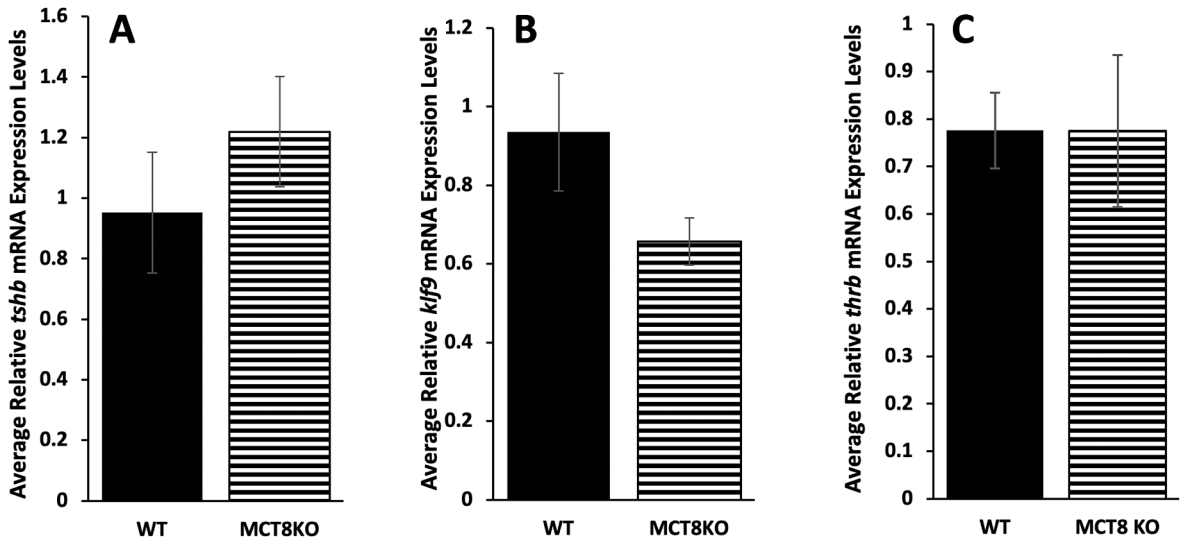

Fig. 5. Gene expression of *tshb*, *klf9*, and *thrb* in the brain at metamorphic climax among MCT8 genotypes. Genotyped F3 tadpoles were reared to metamorphic climax (NF 62), then brain including the pituitary was harvested and processed for quantitative PCR to measure RNA expression of the pituitary gene (A) thyroid stimulating hormone beta (*tshb*) and the TH response genes, (B) Krüppel-like factor 9 (*klf9*) and (C) TH receptor beta (*thrb*). Means and standard error for each genotype are shown, n = 7 for wild-type (WT, LLss), 9 for homozygous MCT8 knockout (MCT8KO, llss). No statistical differences were found using one-way ANOVA, $p < 0.5$.

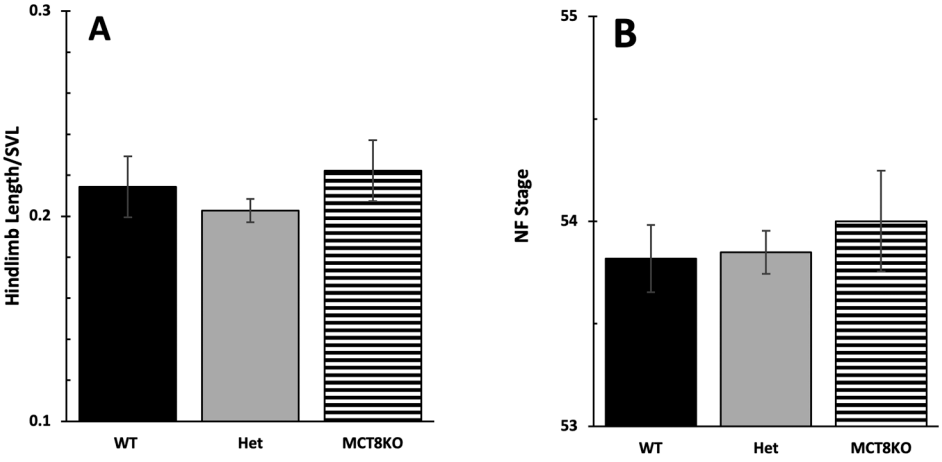

Fig. 6. Initiation of metamorphosis among MCT8 genotypes. To detect an effect of MCT8 on the initiation of metamorphosis, we examined start of limb outgrowth (NF 54) with respect to tadpole size. 79 tadpoles were measured for snout-vent length (SVL) and staged according to Nieuwkoop and Faber (NF) at 21 days post fertilization followed by genotyping. We compared (A) hindlimb length normalized to SVL and (B) NF stage among genotypes. Means and standard error for each genotype are shown, n = 14 for wild-type (WT, LLss), 53 for heterozygous (Het, Llss), 12 for homozygous MCT8 knockout (MCT8KO, llss). No statistical differences were found using one-way ANOVA, $p < 0.5$.

We further examined MCT8 mutant tadpoles for potential effects on TH-dependent developmental timing. The number of possible MCT8 genotypes involving mutant and wild-type MCT8 alleles in the L- and S-chromosomes, i.e., 9 combinations, made it impractical to examine all of them. To reduce the number of genotypes, we decided to focus on varying alleles on the L-chromosome while having both S-chromosome alleles mutant. The S-chromosome MCT8 locus is not expressed as highly or in as many tissues in adults as in the L-chromosome MCT8 locus (Fig. 2), such that loss of *slc16a2.S* would be expected to be less severe compared to loss of *slc16a2.L*. We found no difference in overall rate of metamorphosis among genotypes examined. Plasma TH levels, which are controlled by pituitary TSH action on the thyroid gland, are positively correlated with rate of metamorphosis, and thus the similar *tshb* expression observed here among MCT8 genotypes is consistent with their similar development rates. It is possible that doubly wild-type compared to doubly homozygous mutant MCT8 on L- and S-chromosomes would have given significant differences in our experiment. However, it remains the case that a complete MCT8 double knockout had no effect that we could observe on external morphology or development rate, in contrast to that seen in human or zebrafish (de Vrieze et al., 2014; van Geest et al., 2021).

Regardless of overall developmental rate, examination of individual tissues may reveal an effect on altered TH sensitivity, as seen previously when the expression level of other proteins that affect TH sensitivity were altered (Choi et al., 2015; Huang et al., 1999; Nakajima et al., 2012). In our case, tissues that are very sensitive to TH and have high MCT8 expression levels, such as hindlimbs, may be more affected by MCT8 loss, especially compared to other tissues, such as tail which may not require as high TH sensitivity because it resorbs at the end of metamorphosis when plasma TH levels are maximal. We compared hindlimb and tail sensitivity to exogenous TH and found that both tissues from MCT8 mutant tadpoles showed the same induction of the investigated TH response genes at all doses of TH compared to their wild-type siblings. The one exception was the MCT8 mutant hindlimb had higher *thrb* induction at the highest TH dose compared to wild type, a result that is not understood but does not show that loss of MCT8 reduced tissue sensitivity to TH. Consistent with these results from induced metamorphosis, we observed brain levels of the TH response genes *thrb* and *klf9* at climax of metamorphosis were not affected by the MCT8 mutation. Thus, we did not detect an effect on TH-dependent gene expression or developmental rate from loss of MCT8.

In mice and humans with MCT8 deficiency, whether or not there was

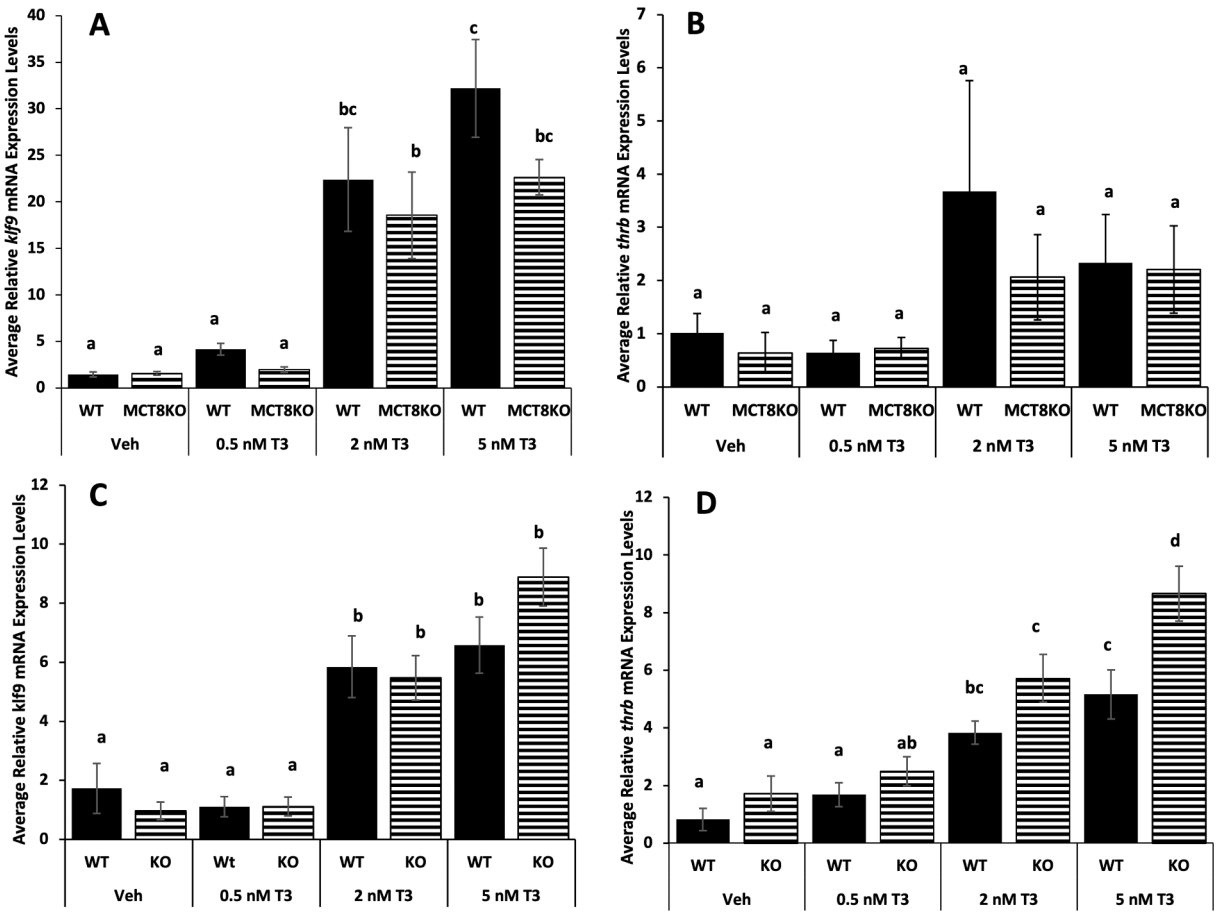

Fig. 7. Tissue sensitivity to TH in tail and hindlimbs among MCT8 genotypes. Premetamorphic F3 tadpoles (NF 54) were treated for 24 hrs with 0, 0.5, 2, and 5 nM T3 (tri-iodothyronine) added to their rearing water, and then their tails and hindlimbs were harvested and processed for quantitative PCR. The RNA expression of the TH response genes, (A,C) Krüppel-like factor 9 (*klf9*) and (B, D) TH receptor beta (*thrb*) in tail (A,B) and hindlimbs (B,C) among MCT8 genotypes. Means and standard error for each genotype are shown, n = 10 for all genotypes and T3 treatments. WT = wild-type (LLss), MCT8KO = homozygous knockout (llss). Letters indicate significant differences among bars determined for each genotype based on non-parametric Kruskal-Wallis test followed by pairwise comparisons using Wilcoxon rank sum exact test (A, B and D) and two-way ANOVA followed by pairwise comparisons using Tukey's post hoc test (C). $p < 0.05$.

a neurological phenotype, TH physiology exhibited high plasma T3 and low plasma T4 with TSH levels in the high normal range (Groeneweg et al., 2020; Trajkovic et al., 2007). Like humans and not mice, zebrafish treated with morpholinos to knock down MCT8 expression had severe brain and spinal cord defects, though plasma TH levels were not measured (Campinho et al., 2014; Vatine et al., 2013). In frogs, no neurobehavioral defect was evident, though a more detailed study may detect some. Also, despite similar rate of external morphological development and similar observed *tshb*, *thrb*, and *klf9* expression, further studies may reveal altered HPT axis regulation and TH response gene expression in some tissues or stages. The different effects of MCT8 deficiency on morphology, behavior, and TH physiology among vertebrates extends the view that expression of TH transporters in tissues important for TH-dependent development varies among species (Vancamp and Darras, 2018).

5. Data availability

All data sets generated during and analyzed during the present study are not publicly available but are available from the corresponding author on reasonable request.

CRediT authorship contribution statement

Zachary R. Sterner: Investigation, Supervision, Visualization. **Ayah Jabrah:** Investigation. **Nikko-Ideen Shaidani:** Investigation, Methodology, Writing – review & editing. **Marko E. Horb:** Conceptualization, Funding acquisition, Project administration, Supervision, Supervision. **Rejenae Dockery:** Investigation. **Bidisha Paul:** Formal analysis, Supervision, Writing – review & editing, Visualization. **Daniel R. Buchholz:** Conceptualization, Funding acquisition, Methodology, Project administration, Supervision, Writing – original draft, Writing – review & editing.

Declaration of Competing Interest

The authors declare that they have no known competing financial interests or personal relationships that could have appeared to influence the work reported in this paper.

Data availability

Data will be made available on request.

Acknowledgement

This work was supported by a Weimann Wendel Benedict grant from the Department of Biological Sciences, University of Cincinnati awarded to ZRS, the National Institutes of Health Grants R24OD030008, P40OD010997 to MEH, and National Science Foundation Grant IOS

2035732 to DRB.

References

Baker, B.S., Tata, J.R., 1992. Prolactin prevents the autoinduction of thyroid hormone receptor mRNAs during amphibian metamorphosis. Dev. Biol. 149, 463–467.

Bernal, J., Guadaño-Ferraz, A., Morte, B., 2015. Thyroid hormone transporters—functions and clinical implications. Nat. Rev. Endocrinol. 11, 406–417.

Bradford, Y.M., Van Slyke, C.E., Ruzicka, L., Singer, A., Eagle, A., Fashena, D., Howe, D. G., Frazer, K., Martin, R., Paddock, H., Pich, C., Ramachandran, S., Westerfield, M., 2022. Zebrafish information network, the knowledgebase for Danio rerio research. Genetics (Austin) 220.

Brown, D.D., Cai, L., Das, B., Marsh-Armstrong, N., Schreiber, A.M., Juste, R., 2005. Thyroid hormone controls multiple independent programs required for limb development in Xenopus laevis metamorphosis. Proc. Natl. Acad. Sci. U. S. A. 102, 12455–12458.

Campinho, M.A., Saraiva, J., Florindo, C., Power, D.M., 2014. Maternal Thyroid Hormones Are Essential for Neural Development in Zebrafish. Mol. Endocrinol. (Baltimore Md.) 28, 1136–1149.

Choi, J., Moskalik, C.L., Ng, A., Matter, S.F., Buchholz, D.R., 2015. Regulation of thyroid hormone-induced development in vivo by thyroid hormone transporters and cytosolic binding proteins. Gen. Comp. Endocrinol. 222, 69–80.

Combes, D., Sillar, K.T., Simmers, J., 2021. Chapter 8: Xenopus frog metamorphosis: A model for studying locomotor network development and neuromodulation. In: Whelan, P.J., Sharples, S.A. (Eds.), The Neural Control of Movement. Academic Press, pp. 175–203.

Connors, K.A., Korte, J.J., Anderson, G.W., Degitz, S.J., 2010. Characterization of thyroid hormone transporter expression during tissue-specific metamorphic events in Xenopus tropicalis. Gen. Comp. Endocrinol. 168, 149–159.

de Vrieze, E., van de Wiel, S.M.W., Zethof, J., Flik, G., Klaren, P.H.M., Arjona, F.J., 2014. Knockdown of Monocarboxylate Transporter 8 (mct8) Disturbs Brain Development and Locomotion in Zebrafish. Endocrinology (Philadelphia) 155, 2320–2330.

Denver, R.J., 2009. Stress hormones mediate environment-genotype interactions during amphibian development. Gen. Comp. Endocrinol. 164, 20–31.

Denver, R.J., 2017. 2.09 - Endocrinology of Complex Life Cycles: Amphibians. In: Anonymous Hormones, Brain, and Behavior, 3rd ed. Elsevier, Amsterdam, pp. 145–168.

Denver, R.J., Pavgi, S., Shi, Y., 1997. Thyroid Hormone-dependent Gene Expression Program for *Xenopus* Neural Development. J 272, 8179-8188.

Dhorne-Pollet, S., Thélie, A., Pollet, N., 2013. Validation of novel reference genes for RT-qPCR studies of gene expression in Xenopus tropicalis during embryonic and post-embryonic development. Dev. Dyn. 242, 709–717.

Dodd, M.H.I., Dodd, J.M., 1976. The biology of metamorphosis. In: Lofts, B. (Ed.), Physiology of the Amphibia. Academic Press, New York, pp. 467–599.

Friesema, E.C.H., Visser, W.E., Visser, T.J., 2010. Genetics and phenomics of thyroid hormone transport by MCT8. Mol. Cell. Endocrinol. 322, 107–113.

Gagnon, J.A., Valen, E., Thyme, S.B., Huang, P., Akhmetova, L., Ahkmetova, L., Pauli, A., Montague, T.G., Zimmerman, S., Richter, C., Schier, A.F., 2014. Efficient Mutagenesis by Cas9 Protein-Mediated Oligonucleotide Insertion and Large-Scale Assessment of Single-Guide RNAs. PLoS One 9, e98186.

Groeneweg, S., Kersseboom, S., van den Berge, A., Dolcetta-Capuzzo, A., van Geest, F.S., van Heerebeek, R.E.A., Arjona, F.J., Meima, M.E., Peeters, R.P., Visser, W.E., Visser, T.J., 2019. Vitro Characterization of Human, Mouse, and Zebrafish MCT8 Orthologues. Thyroid (New York, N.Y.) 29, 1499–1510.

Groeneweg, S., van Geest, F., Peeters, R., Heuer, H., Visser, E., 2020. Thyroid Hormone Transporters. Endocr. Rev. 41, 146–201.

Hellsten, U., Harland, R.M., Gilchrist, M.J., Hendrix, D., Jurka, J., Kapitonov, V., Ovcharenko, I., Putnam, N.H., Shu, S., Taher, L., Blitz, I.L., Blumberg, B., Dichmann, D.S., Dubchak, I., Amaya, E., Detter, J.C., Fletcher, R., Gerhard, D.S., Goodstein, D., Graves, T., Grigoriev, I.V., Grimwood, J., Kawashima, T., Lindquist, E., Lucas, S.M., Mead, P.E., Mitros, T., Ogino, H., Ohta, Y., Poliakov, A.V., Pollet, N., Robert, J., Salamov, A., Sater, A.K., Schmutz, J., Terry, A., Vize, P.D., Warren, W.C., Wells, D., Wills, A., Wilson, R.K., Zimmerman, L.B., Zorn, A.M., Grainger, R., Grammer, T., Khokha, M.K., Richardson, P.M., Rokhsar, D.S., 2010. The genome of the Western clawed frog Xenopus tropicalis. Science 328, 633–636.

Huang, H., Marsh-Armstrong, N., Brown, D.D., 1999. Metamorphosis is inhibited in transgenic Xenopus laevis tadpoles that overexpress type III deiodinase. Proc. Natl. Acad. Sci. U. S. A. 96, 962–967.

Ishizuya-Oka, A., 2017. How thyroid hormone regulates transformation of larval epithelial cells into adult stem cells in the amphibian intestine. Mol. Cell. Endocrinol. 459, 98–103.

Ishizuya-Oka, A., Shimozawa, A., 1994. Inductive action of epithelium on differentiation of intestinal connective tissue of Xenopus laevis tadpoles during metamorphosis in vitro. Cell Tissue Res. 277, 427–436.

Jafkins, A., Abu-Daya, A., Noble, A., Zimmerman, L.B., Guille, M., 2012. Husbandry of Xenopus tropicalis. In: Anonymous Methods in molecular biology (Clifton, N.J.). Humana Press, Totowa, NJ, pp. 17–31.

Just, J.J., Kraus-Just, J., Check, D.A., 1981. Chapter 9: Survey of Chordate Metamorphosis. In: Gilbert, L.I., Frieden, E. (Eds.), MetAmorphosis: A Problem in DevelopmentAl Biology, 2nd ed. Plenum Press, New York, pp. 265–326.

Karimi, K., Fortriede, J.D., Lotay, V.S., Burns, K.A., Wang, D.Z., Fisher, M.E., Pells, T.J., James-Zorn, C., Wang, Y., Ponferrada, V.G., Chu, S., Chaturvedi, P., Zorn, A.M., Vize, P.D., 2018. Xenbase: a genomic, epigenomic and transcriptomic model organism database. Nucl. Acids Res. 46, D861–D868.

Kinne, A., Schülein, R., Krause, G., 2011. Primary and secondary thyroid hormone transporters. Thyroid Res. 4 (Suppl 1), S7.

Kleinau, G., Schweizer, U., Kinne, A., Köhrle, J., Grüters, A., Krude, H., Biebermann, H., 2011. Insights into molecular properties of the human monocarboxylate transporter 8 by combining functional with structural information. Thyroid Res. 4 (Suppl 1), S4.

Leloup, J., Buscaglia, M., 1977. La triiodothyronine, hormone de la metamorphose des Amphibies. C. R. Acad. Sci. Paris Ser. D 284, 2261–2263.

Livak, K.J., Schmittgen, T.D., 2001. Analysis of relative gene expression data using real-time quantitative PCR and the 2(-Delta Delta C(T)) Method. Methods 25, 402–408.

McNamara, S., Wlizla, M., Horb, M.E., 2018. Husbandry, General Care, and Transportation of Xenopus laevis and Xenopus tropicalis. In: Anonymous Methods in molecular biology (Clifton, N.J.). Springer New York, New York, NY, pp. 1–17.

Moreno-Mateos, M.A., Vejnar, C.E., Beaudoin, J., Fernandez, J.P., Mis, E.K., Khokha, M. K., Giraldez, A.J., 2015. CRISPRscan: designing highly efficient sgRNAs for CRISPR-Cas9 targeting in vivo. Nat. Methods 12, 982–988.

Mughal, B.B., Leemans, M., de Souza, E., le Mevel, S., Spirhanzlova, P., Visser, T., Fini, J. B., Demeneix, B.A., 2017. Functional Characterization of Xenopus Thyroid Hormone Transporters mct8 and oatp1c1. Endocrinology (Philadelphia) 158, 2694–2705.

Mukhi, S., Mao, J., Brown, D.D., 2008. Remodeling the exocrine pancreas at metamorphosis in Xenopus laevis. Proc. Natl. Acad. Sci. U. S. A. 105, 8962–8967.

Naert, T., Vleminckx, K., 2018. Genotyping of CRISPR/Cas9 Genome Edited Xenopus tropicalis. In: Vleminckx, K. (Ed.), Methods in molecular biology (Clifton, N.J.). Springer New York, New York, NY, pp. 67–82.

Nakajima, K., Fujimoto, K., Yaoita, Y., 2012. Regulation of thyroid hormone sensitivity by differential expression of the thyroid hormone receptor during Xenopus metamorphosis. Genes Cells 17, 645–659.

Nieuwkoop, P.D., Faber, J., 1994. Normal Table of Xenopus laevis (Daudin). Garland Publishing, New York.

Patmann, M.D., Shewade, L.H., Schneider, K.A., Buchholz, D.R., 2017. Xenopus Tadpole Tissue Harvest. Cold Spring Harb. Protoc. https://doi.org/10.1101/pdb.prot097675.

Pearl, E.J., Grainger, R.M., Guille, M., Horb, M.E., 2012. Development of xenopus resource centers: The national xenopus resource and the European xenopus resource center. Genesis (New York, N.Y: 2000) 25, 155–163.

R Core Team, 2018. R: A language and environment for statistical computing. R Foundation for Statistical Computing, Vienna, Austria. . 3.5. 2.

Salveridou, E., Mayerl, S., Sundaram, S.M., Markova, B., Heuer, H., 2020. Tissue-Specific Function of Thyroid Hormone Transporters: New Insights from Mouse Models. Exp. Clin. Endocrinol. Diabetes 128, 423–427.

Session, A.M., Uno, Y., Kwon, T., Chapman, J.A., Toyoda, A., Takahashi, S., Fukui, A., Hikosaka, A., Suzuki, A., Kondo, M., van Heeringen, S.J., Quigley, I., Heinz, S., Ogino, H., Ochi, H., Hellsten, U., Lyons, J.B., Simakov, O., Putnam, N., Stites, J., Kuroki, Y., Tanaka, T., Michiue, T., Watanabe, M., Bogdanovic, O., Lister, R., Georgiou, G., Paranjpe, S.S., van Kruijsbergen, I., Shu, S., Carlson, J., Kinoshita, T., Ohta, Y., Mawaribuchi, S., Jenkins, J., Grimwood, J., Schmutz, J., Mitros, T., Mozaffari, S.V., Suzuki, Y., Haramoto, Y., Yamamoto, T.S., Takagi, C., Heald, R., Miller, K., Haudenschild, C., Kitzman, J., Nakayama, T., Izutsu, Y., Robert, J., Fortriede, J., Burns, K., Lotay, V., Karimi, K., Yasuoka, Y., Dichmann, D.S., Flajnik, M.F., Houston, D.W., Shendure, J., DuPasquier, L., Vize, P.D., Zorn, A.M., Ito, M., Marcotte, E.M., Wallingford, J.B., Ito, Y., Asashima, M., Ueno, N., Matsuda, Y., Veenstra, G.J., Fujiyama, A., Harland, R.M., Taira, M., Rokhsar, D.S., 2016. Genome evolution in the allotetraploid frog *Xenopus laevis*. Nature 538, 336–343.

Shaidani, N., McNamara, S., Wlizla, M., Horb, M.E., 2020. Animal Maintenance Systems: Xenopus tropicalis. Cold Spring Harbor Protocols pdb.prot106146.

Shi, Y., 1999. Amphibian Metamorphosis: From Morphology to Molecular Biology. Wiley-Liss Inc, New York.

Shi, Y., 2021. Life Without Thyroid Hormone Receptor. Endocrinology (Philadelphia) 162, 1.

Shi, Y.B., Wong, J., Puzianowska-Kuznicka, M., Stolow, M.A., 1996. Tadpole competence and tissue-specific temporal regulation of amphibian metamorphosis: roles of thyroid hormone and its receptors. Bioessays 18, 391–399.

Trajkovic, M., Visser, T., Mittag, J., Horn, S., Lukas, J., Darras, V.M., Raivich, G., Bauer, K., Heuer, H., 2007. Abnormal thyroid hormone metabolism in mice lacking the monocarboxylate transporter 8. J. Clin. Invest. 117, 627–635.

Truett, G.E., Heeger, P., Mynatt, R.L., Truett, A.A., Walker, J.A., Warman, M.L., 2000. Preparation of PCR-Quality Mouse Genomic DNA with Hot Sodium Hydroxide and Tris (HotSHOT). Biotechniques 29, 52–54.

van Geest, F.S., Gunhanlar, N., Groeneweg, S., Visser, W.E., 2021. Monocarboxylate Transporter 8 Deficiency: From Pathophysiological Understanding to Therapy Development. Front. Endocrinol. (Lausanne) 12, 723750.

Vancamp, P., Darras, V.M., 2018. From zebrafish to human: A comparative approach to elucidate the role of the thyroid hormone transporter MCT8 during brain development. Gen. Comp. Endocrinol. 265, 219–229.

Vatine, G.D., Zada, D., Lerer-Goldshtein, T., Tovin, A., Malkinson, G., Yaniv, K., Appelbaum, L., 2013. Zebrafish as a Model for Monocarboxyl Transporter 8-Deficiency. J. Biol. Chem. 288, 169–180.

Visser, W.E., Friesema, E.C., Visser, T.J., 2010. Minireview: Thyroid Hormone Transporters: The Knowns and the Unknowns. Mol. Endocrinol. 25, 1–14.

Wlizla, M., McNamara, S., Horb, M.E., 2018. Generation and Care of Xenopus laevis and Xenopus tropicalis Embryos. In: Anonymous Methods in molecular biology (Clifton, N.J.). Springer New York, New York, NY, pp. 19–32.